Journal of Nuclear Materials 417 (2011) 445–450

Contents lists available at ScienceDirect

Journal of Nuclear Materials

journal homepage: www.elsevier.com/locate/jnucmat

Damage production and accumulation in SiC structures in inertial and magnetic fusion systems

M.E. Sawan [a,*], N.M. Ghoniem [b], L. Snead [c], Y. Katoh [c]

[a] University of Wisconsin-Madison, 1500 Engineering Dr, Madison, WI 53706, USA
[b] University of California-Los Angeles, Los Angeles, CA, USA
[c] Oak Ridge National Laboratory, Oak Ridge, TN, USA

ARTICLE INFO

Article history:
Available online 24 December 2010

ABSTRACT

Radiation damage parameters in SiC/SiC composite structures are determined in both magnetic (MFE) and inertial (IFE) confinement fusion systems. Variations in the geometry, neutron energy spectrum, and pulsed nature of neutron production result in significant differences in damage parameters between the two systems. With the same neutron wall loading, the displacement damage rate in the first wall in an IFE system is ~10% lower than in an MFE system, while gas production and burnup rates are a factor of 2 lower. Self-cooled LiPb and Flibe blankets were analyzed. While using LiPb results in higher displacement damage, Flibe yields higher gas production and burnup rates. The effects of displacement damage and helium production on defect accumulation in SiC/SiC composites are also discussed.

1. Introduction

SiC/SiC composites have been proposed as structural material for the first wall (FW) and blanket in several magnetic (MFE) and inertial (IFE) confinement power plants because of their low induced radioactivity and high temperature operation [1–3]. SiC/SiC composite was selected as a structural material for the recent High Average Power Laser (HAPL) fusion conceptual design with magnetic intervention due to its large electrical resistivity that allows dissipating the magnetic energy resistively [3]. Radiation effects on the fiber, matrix, and interphase must be properly assessed for determination of component lifetime and performance under irradiation. In this paper, we determine the key radiation damage parameters and highlight the significant geometrical, spectral, and temporal differences that exist between IFE and MFE systems. To obtain prototypical neutron damage parameters, we used the configuration of ARIES-AT advanced tokamak [2] as a representative of MFE concepts and the HAPL design [3] to represent IFE environments. Self-cooled blanket concepts with LiPb and Flibe were analyzed. The coolant/breeder choice affects the radiation damage parameters by impacting the neutron flux and spectrum.

2. Calculation model

The damage parameters calculated are atomic displacement rate, gas production rates, and total transmutation or burnup rates. The PARTISN code [4] was used for the steady state or time integrated calculations. Time-dependent neutronics calculations for the pulsed IFE system were performed using MCNP [5]. For the MFE system, the ARIES-AT radial build at mid-plane was used with the inboard (IB) and outboard (OB) regions modeled simultaneously. The model for the LiPb blanket includes a 7-mm thick SiC/SiC structural FW followed by a breeding blanket consisting of 90% LiPb (with 90% ^{6}Li enrichment) and 10% SiC/SiC structure [6]. For the Flibe blanket option, a 10-mm thick Be layer is inserted in the FW coolant channel to achieve adequate tritium breeding [7]. A uniform 14.1 MeV neutron source is used in the plasma zone. In the IFE system, we used the same blanket radial build as that used for the OB region in the MFE system. The calculations were performed in spherical geometry with a point isotropic neutron source emitting neutrons with a softened target energy spectrum at the center of a 4.25 m radius chamber. The HAPL target spectrum [8] was used. The neutron wall loadings in the IFE system and in the OB region of the MFE system were normalized to the same time-average value of 6 MW/m^2.

3. Damage parameters in the MFE system

Table 1 gives the peak radiation damage parameters in the Si and C sub-lattices as well as the average values for SiC at midplane in the OB region for both the LiPb and Flibe blankets. The interphase material candidates are graphite and multilayer SiC. The damage parameters for the SiC interphase material are identical to those for the SiC fiber/matrix. The damage parameters for the graphite interphase material are the same as those for the C sublattice of SiC except for the dpa due to the higher displacement energy of C in graphite. The results indicate that the dpa rate in the C

* Corresponding author. Tel.: +1 608 263 5093; fax: +1 608 263 4499.
E-mail address: sawan@engr.wisc.edu (M.E. Sawan).

0022-3115/$ - see front matter © 2010 Elsevier B.V. All rights reserved.
doi:10.1016/j.jnucmat.2010.12.077

Table 1
Peak damage parameters n MFE and IFE systems.

		dpa/FPY	He appm/FPY	H appm/FPY	% Burnup/FPY
MFE System					
C	LiPb	112	15,858	3	0.64
	Flibe	52	16,633	3	0.68
Si	LiPb	97	4001	7309	1.13
	Flibe	66	4473	8064	1.25
SiC	LiPb	105	9930	3656	1.77
	Flibe	59	10,553	4033	1.93
Graphite	LiPb	75	15,858	3	0.64
	Flibe	35	16,633	3	0.68
IFE System					
C	LiPb	111	7718	5	0.32
	Flibe	45	8096	5	0.35
Si	LiPb	82	2106	3783	0.59
	Flibe	47	2388	4252	0.66
SiC	LiPb	96	4912	1894	0.91
	Flibe	46	5242	2129	1.01
Graphite	LiPb	73	7718	5	0.32
	Flibe	30	8096	5	0.35

sub-lattice is larger than in the Si sub-lattice. The dpa rate in the graphite interphase material is 33% lower than in the C sub-lattice of SiC. The He production rate in the C sub-lattice and the graphite interphase material is about a factor of 4 higher than in the Si sub-lattice and is dominated by the (n,n′3α) reaction. The average He production rate in the graphite interphase is 60% higher than the average He production rate in SiC. Significant hydrogen production occurs in the silicon with a negligible amount produced in the carbon. The burnup rate of the Si sub-lattice is twice that for the C sub-lattice. The importance of determining nuclear transmutation rates stems from the fact that property degradation depends on the level of impurities introduced. Si transmutes primarily to Mg and Al with smaller amount of P while C produces Be with smaller amount of B and Li [9]. The non-stoichiometric burnup of Si and C is expected to be worse than stoichiometric burnups and could be an important issue for lifetime assessment.

Fig. 1 shows the radial variation of the damage parameters of SiC at midplane in the OB region for the LiPb blanket. We note that gas production and burnup due to high-energy neutrons drop faster as one moves deeper in the blanket. The peak parameters in the OB FW for a Flibe blanket given in Table 1 show that the dpa values are about half those obtained with LiPb while the gas production and burnup rates are higher by 3–10%. Flibe is more effective attenuating intermediate energy neutrons, due to slowing down by the low mass Be and F, while LiPb, with its large mass Pb, is more effective attenuating neutrons in the high MeV range that contribute to gas production and burnup. Fig. 2 shows that the dpa rate in the Flibe blanket decreases with distance at a faster rate compared to that in the LiPb blanket while gas production and burnup rates have slightly less steep radial drop. The energy spectra of neutrons at the OB FW for the LiPb and Flibe blankets, given in Fig. 3, show a harder spectrum with Flibe resulting in larger high energy ($E > 2$ MeV) flux, that dominates gas production and burnup, but lower intermediate energy flux (10 keV–2 MeV) that significantly contributes to atomic displacement damage. This results in higher gas production and burnup rates and lower dpa rates in Flibe blanket compared to LiPb blanket.

4. Damage parameters in the IFE system

The peak radiation damage parameters at the FW in the HAPL IFE reactor with LiPb and Flibe blankets are given in Table 1. While the relative values for the constituents show similar trends as in the MFE system, the peak values for the same neutron wall loading are significantly different. Gas production and burnup rates are about a factor of 2 lower in the IFE system. The peak dpa rate in IFE is lower than that in the MFE system by ~7% for LiPb blanket and ~20% for Flibe blanket. Comparing the profiles for damage parameters in the IFE system to those obtained in the OB region of the MFE system indicated that the gradient is much smaller in IFE as shown in Fig. 4 for helium production. This is a direct consequence of the geometrical differences discussed below.

There are significant geometrical, spectral, and temporal differences between MFE and IFE systems that affect the radiation dam-

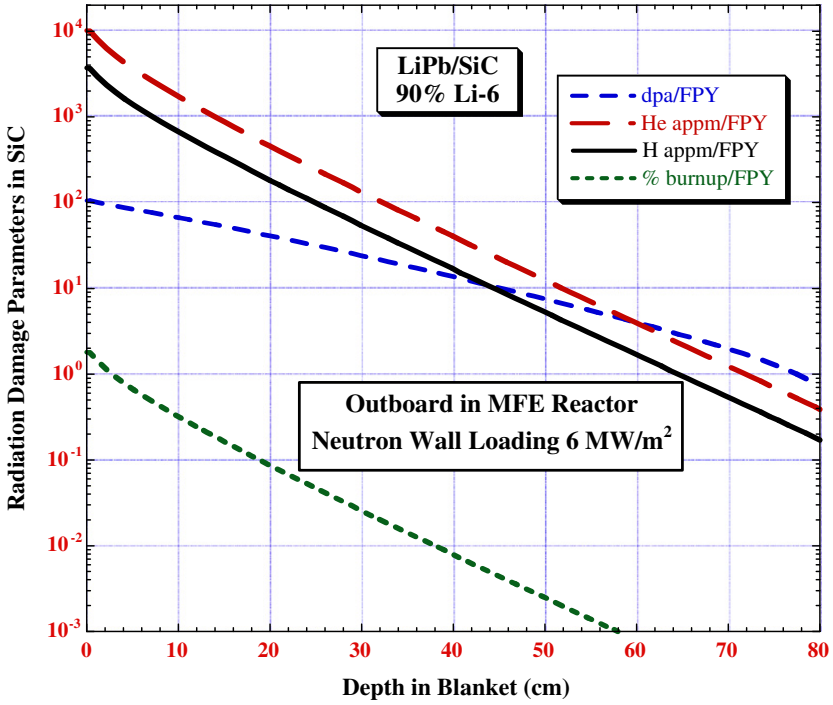

Fig. 1. Radial variation of radiation damage parameters in LiPb OB blanket.

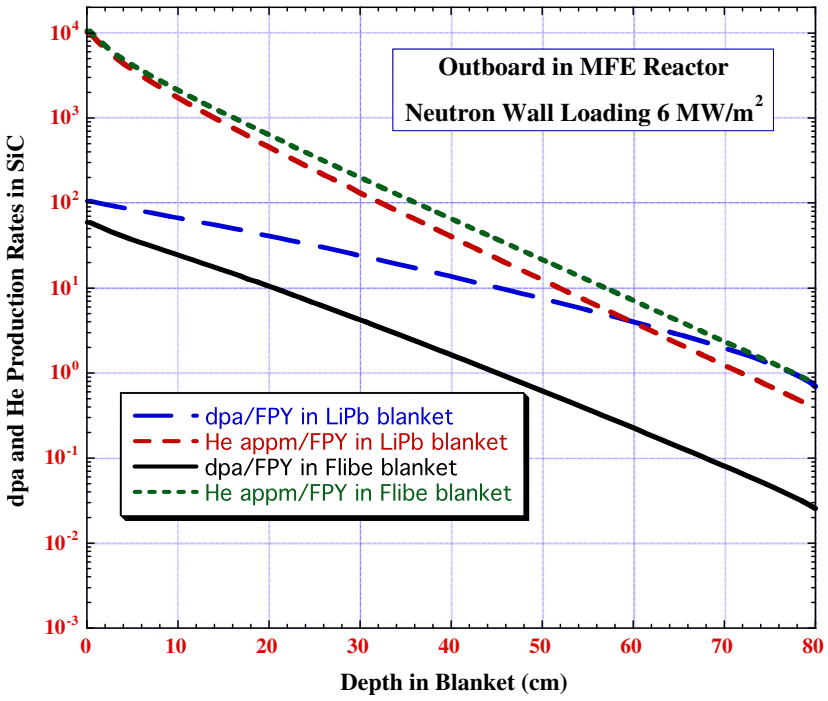

Fig. 2. Radial variations of atomic displacement damage and He production in LiPb and Flibe blankets.

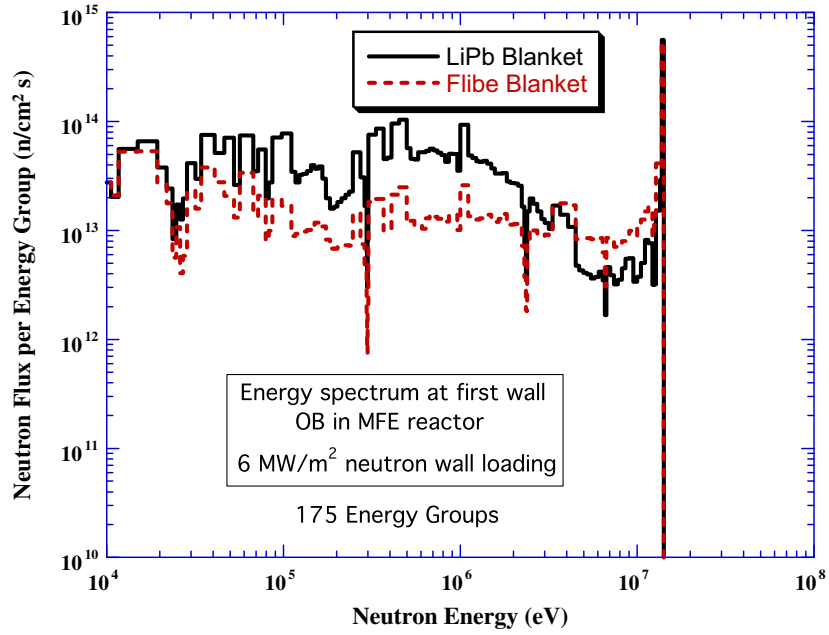

Fig. 3. Comparison between neutron energy spectra at FW in LiPb and Flibe OB blankets.

age levels with impact on lifetime assessment [10]. While a cylindrical or toroidal chamber surrounds a volumetric distributed source in MFE systems, a nearly spherical chamber surrounds a point neutron source in an IFE system. As a result, source neutrons in IFE chambers impinge on the FW/blanket in a more perpendicular direction. This leads to lower FW radiation damage parameters with a smaller radial gradient for the same neutron wall loading. The peak damage parameters in the FW are lower in IFE systems but start to be higher than in MFE system at ~6 cm depth in the blanket. Thus, extrapolation of radiation damage parameters between MFE and IFE fusion energy systems is not possible.

Fusion neutron interactions in the compressed target result in considerable softening of the neutron spectrum incident on the FW/blanket in IFE chambers. While in MFE systems source neutrons incident on the FW are at 14.1 MeV, those incident on the FW of the IFE system have average energies in the range 10–13 MeV. In addition, some neutron multiplication takes place in the target. For each fusion reaction in the HAPL target, 1.05 neutrons are emitted from the target with an average energy of 12.3 MeV. For the same neutron wall loading, the lower average energy of source neutrons in IFE results in a larger number of neutrons impinging directly on the FW as compared to the MFE cham-

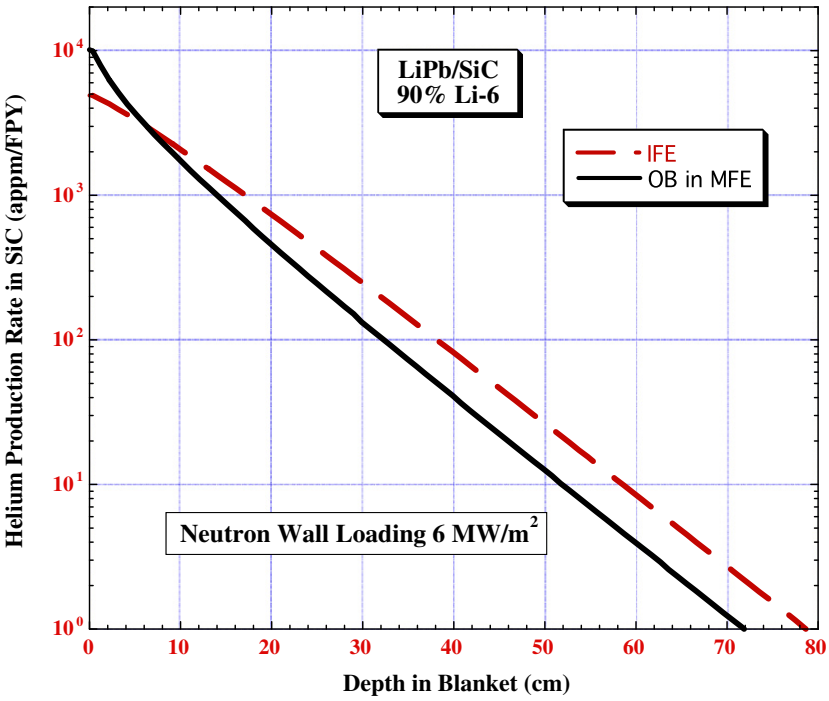

Fig. 4. Comparison between He production rates in MFE and IFE LiPb blankets.

ber. However, these lower energy neutrons produce less secondary neutrons from interactions in the blanket. The net result is comparable neutron fluxes at the FW. While the calculated total neutron flux values at the FW were nearly identical in both systems, the neutron energy spectrum at the FW in the IFE system is softer with an average energy of 1.66 MeV compared to 2.67 MeV in the MFE system. This softer spectrum, combined with the angular difference discussed above, contributes to the observed lower peak damage parameters at the FW in IFE systems.

5. Pulsed radiation damage in IFE systems

In an IFE chamber, the neutron source is pulsed because of the very short burn time (10–100 ps) of the D-T fuel pellet. The softened target neutron energy spectrum results in time of flight spread with most of the neutrons arriving at the FW over a time period of several nanoseconds. The arrival time depends on the chamber radius and is ~80 ns after the D-T pellet burn completion for the HAPL chamber. In addition, backscattering from the blanket extends the period over which damage production takes place. As a result, the time spread of displacement damage is longer than that for gas production and transmutation rates [11]. Fig. 5 shows the instantaneous atomic displacement damage rate as a function of time following the burn in the FW of the HAPL IFE system that utilizes a LiPb blanket. Table 2 lists the temporal peaks, peaking factor, and time integrated damage parameters for both LiPb and Flibe blankets.

The temporal peaking factor is significantly higher (by up to an order of magnitude) for He production than for atomic displacements. This is due to the fact that neutrons scattered back from the blanket at later times are low in energy and contribute to atomic displacement without a corresponding contribution to gas production. This leads to the peak instantaneous He/dpa ratio being much higher than that determined from the temporal average (cumulative) values (368 compared to 47). The peaking factor for dpa in a Si sub-lattice is about a factor of 2 higher than that for the C sub-lattice. While peak instantaneous dpa values are comparable for the Flibe and LiPb blankets, the peaking factor for dpa in the Flibe blanket is higher (by a factor of ~2) than that in the LiPb blanket due to increased low energy neutrons scattered back from LiPb. On the other hand, peak values as well as peaking factors for He production are comparable for Flibe and LiPb blankets since low energy scattered back neutrons have negligible contribution to He production.

6. Defect production in SiC/SiC composites

The strong directional bonding and the mass difference between Si and C atoms render the crystalline form of β-SiC exceptional radiation resistance characteristics. Molecular dynamics (MD) studies [12] show that replacement collision sequences (RCSs) are improbable, and that the displacement of C atoms is much easier than Si. As a result, the stoichiometry of displacement cascades will differ substantially from that of the matrix. It is also observed that energetic Si PKAs displace multiple C atoms which end up on {1 1 1} planes. Thus, C-rich interstitial dislocation loops will tend to form on {1 1 1} planes. Haung and Ghoniem [13] determined neutron partial displacement cross sections, displacement cross sections in each sub-lattice, and for each PKA type in SiC. The corresponding damage rates for several fusion and fission neutron spectra were calculated, and the stoichiometry of irradiated SiC was investigated by finding the ratio of displacements among various atomic species. Their study showed that neutron displacement damage rates of SiC in typical MFE FW to be 10–15 dpa MW^{-1} m^2, while in typical LiPb-protected IFE FW, the damage rate is in the range 15–20 dpa MW^{-1} m^2. Approximately 80% of displacement atoms were shown to be of the carbon-type.

Vacancies and He atoms exhibit considerable mobility above 1000 °C. Price [14] observed Frank-type loops on {1 1 1} planes which may be C-rich. Below 1000 °C, point defects tend to form loops on {1 1 1} planes and swelling is therefore expected to saturate. For example, Harrison and Corelli [15] observed large loops (10–200 nm) in β-SiC after neutron irradiation to a fluence of 1.8×10^{23} cm^{-2}. At temperatures above 1000 °C, cavities form, and swelling does not saturate. The presence of helium results in

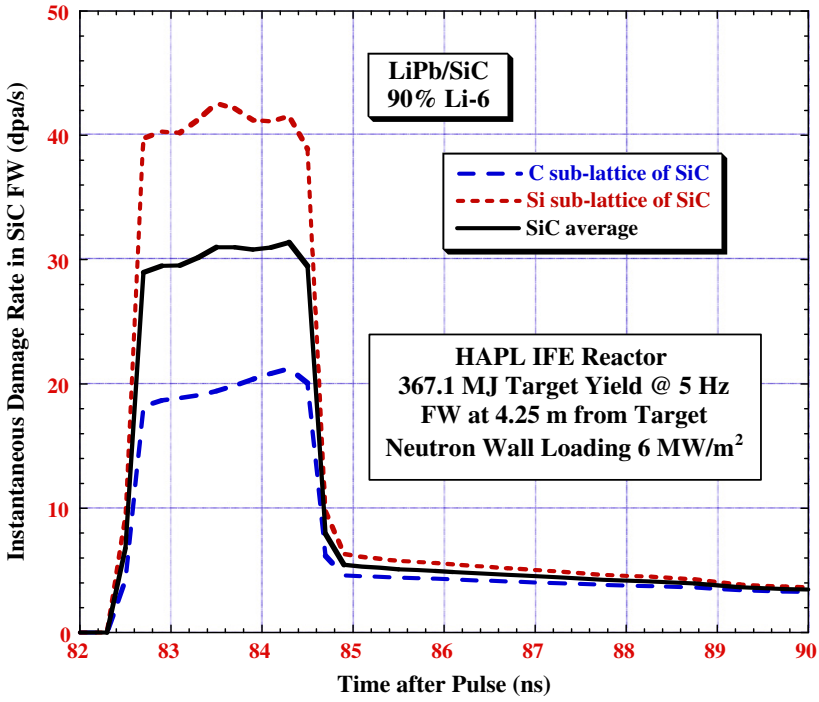

Fig. 5. Instantaneous damage rate in SiC FW for LiPb blanket.

Table 2
Temporal peak and average values for instantaneous damage parameters.

		Temporal peak	Time average	Peak/average
dpa/s				
C	LiPb	21.25	3.24×10^{-6}	6.6×10^{6}
	Flibe	20.56	1.23×10^{-6}	1.7×10^{7}
Si	LiPb	42.58	2.35×10^{-6}	1.8×10^{7}
	Flibe	42.50	1.27×10^{-6}	3.4×10^{7}
SiC	LiPb	31.39	2.80×10^{-6}	1.1×10^{7}
	Flibe	30.96	1.25×10^{-6}	2.5×10^{7}
He appm/s				
C	LiPb	18,410	2.02×10^{-4}	9.1×10^{7}
	Flibe	18,410	2.05×10^{-4}	9.0×10^{7}
Si	LiPb	4404	5.96×10^{-5}	7.4×10^{7}
	Flibe	4410	6.48×10^{-5}	6.8×10^{7}
SiC	LiPb	11,407	1.31×10^{-4}	8.7×10^{7}
	Flibe	11,410	1.35×10^{-4}	8.5×10^{7}

further increases in the swelling rate by the well-known gas-driven swelling mechanism.

7. Lifetime considerations

The useful lifetime of SiC/SiC composites in a fusion neutron environment presently is only speculated, as discussed in a previous paper [16]. The development work to date has determined that the most radiation resistant SiC composites are manufactured from essentially stoichiometric fiber, matrix, and interphase [17] and these constituents behave under irradiation essentially as pure SiC. Moreover, for the highest dose irradiation carried out to date it appears that fission neutron cascade damage may not in itself be a life-limiting factor for SiC [18]. However, the production of He and metallic transmutants produced through fusion neutron interaction may well prove life limiting. Transmutations will likely produce an unbalanced stoichiometry, and depending on the irradiation temperature, this may result in significant microstructural changes. Moreover, and again depending on temperature, the presence of copious amounts of transmuted helium along with irradiation-produced vacancies may also result in microstructural and volumetric change. Loss of strength is expected due to helium bubble formation at the grain boundaries or the presence of low-melting metallic transmutation products. The magnitude of swelling or the overall impact of the transmutation products on strength is not presently understood. As facilities are not currently available to experimentally simulate the fusion neutron environment an active modeling activity in this area is sought.

One of the key features of radiation damage in IFE is the extremely high instantaneous displacement damage rate as compared to MFE irradiation. Such high damage rate results in enhanced point defect recombination during the on-time, followed by annealing of defects during the off-time [11]. As a result, the microstructure can be vastly different as compared to MFE. At high temperatures, and during the off-time of the radiation pulse, the accumulated defects may undergo annealing. For example, it has been shown that void swelling in steels can be partially suppressed under IFE conditions as a result of high temperature effects on annealing of voids [19]. Another difference that should be taken into account in IFE systems is that damage from X-rays, neutrons and ion debris occur over different time scales unlike in MFE systems. It is therefore essential to account for these unique features for accurate prediction of the structure lifetime in IFE systems.

8. Summary and conclusions

We determined here radiation damage parameters for SiC/SiC composites in both MFE and IFE confinement systems. Significant geometrical, spectral, and pulsed differences are shown to exist between the two systems. The configurations of ARIES-AT and HAPL were used for MFE and IFE concepts, respectively. Self-cooled blanket concepts with LiPb and Flibe were analyzed. Values of dpa, gas production, and burnup were determined and compared. With the same neutron wall loading, the first wall dpa in IFE is ~10% lower than in MFE and gas production and burnup are a factor of 2 lower. This is due to the perpendicular incidence of source neutrons and the softer neutron spectrum in IFE.

Production of lattice defects in SiC results in non-stoichiometric displacements of Si and C atoms, which in turn can result in changes in the local chemistry and a wide variety of lattice defects. Point defects form on the sub-lattices of C and Si independently. Additionally, Si and C atoms can switch positions forming anti-site defects. Furthermore, the pulsed nature of IFE results in extremely high instantaneous damage production rates as high as ~40 dpa/s. The ratio of instantaneous-to-average dpa rate is about 50 million, with implications to the accumulation of surviving defects. In addition, the time spread of displacement damage production is longer than that for helium production leading to peak instantaneous He/dpa ratio that is higher than the average value. The strong directional bonding and the mass difference between Si and C atoms result in unique displacement features in SiC as compared to metals. The useful lifetime of SiC/SiC composites in a fusion neutron environment depends on the magnitude of swelling and the overall impact of the transmutation products on strength that are not presently understood. As facilities are not currently available to experimentally simulate the fusion neutron environment, active modeling and experimental activities in this area will provide significant insight into the physics of damage production and accumulation in SiC/SiC composites.

Acknowledgement

Funding for this work was provided through grants from the US Department of Energy.

References

[1] R. Raffray, R. Jones, G. Aiello, et al., Fus. Eng. Des. 55 (2001) 55–95.
[2] F. Najmabad, the ARIES Team, Fus. Eng. Des. 80 (2006) 3–23.
[3] J. Sethian et al., J. Nucl. Mater. 347 (2005) 161–177.
[4] R.E. Alcouffe, R.S. Baker, J.A. Dahl, et al., "PARTISN: A Time-Dependent, Parallel Neutral Particle Transport Code System", LA-UR-05-3925, May 2005.
[5] X-5 Monte Carlo Team, "MCNP-A General Monte Carlo N-Particle Transport Code, Version 5-Volume II: Users Guide", LA-CP-03-0245, April 2003, revised February2008.
[6] M.E. Sawan, C.S. Aplin, G. Sviatoslavsky, I.N. Sviatoslavsky, A.R. Raffray, Fus. Sci. Technol. 52 (2007) 771–775.
[7] M.E. Sawan, C.S. Aplin, G. Sviatoslavsky, A.R. Raffray, "Neutronics Analysis of a Molten Salt Blanket for the HAPL Laser Fusion Power Plant with Magnetic Intervention", in: Proceedings of the 22nd IEEE/NPSS Symposium on Fusion Engineering (SOFE), June 17–21, 2007, Albuquerque NM.
[8] L.J. Perkins, "HAPL Reactor Targets: Baseline Specifications and Future Options", available at http://aries.ucsd.edu/HAPL/DOCS/HAPLtargetSpecs.pdf.
[9] M. Sawan, E. Marriott, M. Dagher, "Neutronics Performance Parameters for the US Dual Coolant Lead Lithium ITER Test Blanket Module", in: Proceedings of the 23rd IEEE/NPSS Symposium on Fusion Engineering (SOFE), May 31–June 5, 2009, San Diego, CA.
[10] M. Sawan, Fus. Technol. 10 (1986) 1483–1488.
[11] M. Sawan, G. Kulcinski, N. Ghoniem, J. Nucl. Mater. 103 (1981) 109–113.
[12] A. El-Azab, N. Ghoniem, J. Nucl. Mater. 191–194 (1992) 1110–1113.
[13] H. Haung, N.M. Ghoniem, J. Nucl. Mater. 199 (1993) 221–230.
[14] R.J. Price, J. Nucl. Mater. 46 (1973) 268–272.
[15] S.D. Harrison, J.C. Corelli, J. Nucl. Mater. 122&123 (1984) 833–839.
[16] M. Sawan, L. Snead, S. Zinkle, Fus. Sci. Technol. 44 (2003) 150–154.
[17] G. Newsome, L.L. Snead, T. Hinoki, Y. Katoh, D. Peters, J. Nucl. Mater. 371 (2007) 76–89.
[18] L.L. Snead, T. Nozawa, Y. Katoh, et al., J. Nucl. Mater. 371 (2007) 329–377.
[19] N.M. Ghoniem, G.L. Kulcinski, J. Nucl. Mater. 69–70 (1978) 816–820.